Drastic reduction of sarcalumenin in Dp427 (dystrophin of 427 kDa)-deficient fibres indicates that abnormal calcium handling plays a key role in muscular dystrophy

Paul DOWLING, Philip DORAN and Kay OHLENDIECK[1]

Department of Biology, National University of Ireland, Maynooth, County Kildare, Ireland

Although the primary abnormality in dystrophin is the underlying cause for mdx (X-chromosome-linked muscular dystrophy), abnormal Ca^{2+} handling after sarcolemmal microrupturing appears to be the pathophysiological mechanism leading to muscle weakness. To develop novel pharmacological strategies for eliminating Ca^{2+}-dependent proteolysis, it is crucial to determine the fate of Ca^{2+}-handling proteins in dystrophin-deficient fibres. In the present study, we show that a key luminal Ca^{2+}-binding protein SAR (sarcalumenin) is affected in mdx skeletal-muscle fibres. One- and two-dimensional immunoblot analyses revealed the relative expression of the 160 kDa SR (sarcoplasmic reticulum) protein to be approx. 70 % lower in mdx fibres when compared with normal skeletal muscles. This drastic reduction in SAR was confirmed by immunofluorescence microscopy. Patchy internal labelling of SAR in dystrophic fibres suggests an abnormal formation of SAR domains. Differential co-immunoprecipitation experiments and chemical cross-linking demonstrated a tight linkage between SAR and the SERCA1 (sarcoplasmic/endoplasmic-reticulum Ca^{2+}-ATPase 1) isoform of the SR Ca^{2+}-ATPase. However, the relative expression of the fast Ca^{2+} pump was not decreased in dystrophic membrane preparations. This implies that the reduction in SAR and calsequestrin-like proteins plays a central role in the previously reported impairment of Ca^{2+} buffering in the dystrophic SR [Culligan, Banville, Dowling and Ohlendieck (2002) J. Appl. Physiol. **92**, 435–445]. Impaired Ca^{2+} shuttling between the Ca^{2+}-uptake SERCA units and calsequestrin clusters via SAR, as well as an overall decreased luminal ion-binding capacity, might indirectly amplify the Ca^{2+}-leak-channel-induced increase in cytosolic Ca^{2+} levels. This confirms the idea that abnormal Ca^{2+} cycling is involved in Ca^{2+}-induced myonecrosis. Hence, manipulating disturbed Ca^{2+} handling might represent new modes of abolishing proteolytic degradation in muscular dystrophy.

Key words: calcium handling, Dp427 (dystrophin of 427 kDa), dystrophin, muscular dystrophy, sarcalumenin.

INTRODUCTION

Ca^{2+} ions are involved in the fine regulation of numerous physiological processes. The highly organized interactions between Ca^{2+} channels, Ca^{2+}-sequestrating proteins and Ca^{2+} pumps maintain the precise temporal and spatial control of Ca^{2+} fluxes, Ca^{2+} buffering and Ca^{2+} uptake [1]. The importance of Ca^{2+} handling for signal transduction has been well established for muscle tissues [2]. Ca^{2+} cycling through the SR (sarcoplasmic reticulum) regulates the contractile status of skeletal-muscle fibres, making Ca^{2+} ions key second-messenger molecules of the excitation–contraction–relaxation cycle [3]. In mdx (X-chromosome-linked muscular dystrophy), a neuromuscular disorder caused by the primary deficiency in the membrane cytoskeletal protein Dp427 (dystrophin of 427 kDa) [4], abnormal Ca^{2+} handling has been postulated to play a major role in the secondary steps leading to fibre necrosis [5]. It is well established that the primary deficiency in dystrophin and the secondary reduction in the dystrophin-associated glycoprotein complex lead to an impaired linkage between the actin membrane cytoskeleton and the extracellular matrix component LAM (laminin) [6,7]. Loss of sarcolemmal integrity is believed to render the muscle periphery more susceptible to microrupturing [8], thereby allowing for the insertion of Ca^{2+}-leak channels into the sarcolemma during the natural processes of cell-membrane resealing [5].

Although the recent analysis of transgenic mdx muscles exhibiting an overexpression of utrophin suggests that mechanosensitive Ca^{2+} channels are not the initial triggering factors of the dystrophic process [9], their presence clearly gives rise to localized Ca^{2+} increases near the sarcolemma [10]. This contributes a cycle of enhanced protease activity and Ca^{2+}-leak channel activation [11]. The pathophysiological modification of ion-regulatory surface elements may precede the increased Ca^{2+}-leak channel activation, which is then followed by downstream alterations in the intracellular Ca^{2+}-handling apparatus. Recent studies suggest the involvement of Ca^{2+}-permeable growth-factor-regulated channels [12] and transient receptor potential channels [13] in Ca^{2+} fluxes through the dystrophic sarcolemma. In contrast, the involvement of the voltage-sensing dihydropyridine receptor of the transverse tubules [14] or potential abnormalities in the formation of the Ca^{2+}-release channel complex [15] have been excluded as major factors in muscular dystrophy.

On the basis of a recent survey of the fate of Ca^{2+}-regulatory membrane proteins in dystrophin-deficient muscle membranes [16], we have extended our immunoblot analysis to the Ca^{2+}-binding element SAR (sarcalumenin) [17]. Within the SR lumen, loss of the CLPs [CSQ (calsequestrin)-like proteins] [16], indicative of impaired CSQ clustering [18], may contribute to decreased luminal Ca^{2+} buffering. This probably amplifies the increased free cytosolic Ca^{2+} levels. In analogy, abnormal

Abbreviations used: CSQ, calsequestrin; CLP, CSQ-like protein; DAPI, 4,6-diamidino-2-phenylindole; DG, dystroglycan; Dp427, dystrophin of 427 kDa; DTSP, dithiobis(succinimidyl propionate); DTT, dithiothreitol; HRC, histidine-rich Ca^{2+}-binding protein; IEF, isoelectric focusing; IPG, immobilized pH gradient; mAb, monoclonal antibody; LAM, laminin; mdx, X-chromosome-linked muscular dystrophy; SAR, sarcalumenin; SERCA, sarcoplasmic/endoplasmic-reticulum Ca^{2+}-ATPase; SR, sarcoplasmic reticulum; 53-SRGP, SR glycoprotein of 53 kDa; Up395, utrophin of 395 kDa.

[1] To whom correspondence should be addressed (e-mail kay.ohlendieck@may.ie).

expression patterns of other luminal Ca^{2+}-binding proteins might also be involved in this process. SAR of 160 kDa apparent mass binds approx. 35 mol of Ca^{2+} ions per mol of protein and is located in both the longitudinal tubules and the terminal cisternae region of the SR [19]. SAR is expressed at comparable levels in predominantly slow- and fast-twitching muscle fibres [20]. Although almost all key Ca^{2+}-regulatory membrane proteins undergo isoform switching after chronic low-frequency stimulation [21], the relative expression levels of SAR are not altered during stimulation-induced fast- to slow-fibre transitions [20].

mAb (monoclonal antibody) XIIC4 to SAR recognizes 53-SRGP (SR glycoprotein of 53 kDa) in addition to the main 160 kDa band [22]. The 53 kDa protein does not bind Ca^{2+} ions and represents an alternative splice variant of the C-terminal part of the SAR gene [17]. Comparative immunoelectron microscopy has demonstrated that both proteins co-localize with the SR Ca^{2+}-ATPase [19]. Studies by Shoshan-Barmatz et al. [23,24] suggest that cycles of phosphorylation and dephosphorylation of SAR and HRC (histidine-rich Ca^{2+}-binding protein) modulate the activity of the junctional ryanodine receptor Ca^{2+}-release channel complex. In addition, other endogenous regulators of the ryanodine receptor are represented by triadin and CSQ [25].

The present study demonstrates that SAR is reduced in dystrophic SR vesicles, supporting the previous observation that dystrophic fibres exhibit impaired luminal Ca^{2+} buffering [16], in addition to increased cytosolic Ca^{2+} levels [5,10,11]. Furthermore, the idea that disturbed ion homoeostasis is a key pathobiochemical factor that triggers Ca^{2+}-induced myonecrosis agrees with recent studies showing that the pharmacological elimination of Ca^{2+}-dependent proteolysis counteracts dystrophic changes in muscle cells [26,27].

MATERIALS AND METHODS

Materials

Ultrapure Protogel acrylamide stock solutions were obtained from National Diagnostics (Atlanta, GA, U.S.A.) and protease inhibitors from Roche Diagnostics (Mannheim, Germany). Chemiluminescence substrates and the Seize-X™ Protein A immunoprecipitation kit were purchased from Perbio Science U.K. (Tattenhall, Cheshire, U.K.). Protran nitrocellulose membranes were obtained from Schleicher and Schuell (Dassel, Germany) and IPG (immobilized pH gradient) strips (pH 3–10) and IPG buffer (pH 3–10) from Amersham Biosciences (Little Chalfont, Bucks., U.K.). The cationic carbocyanine dye 'Stains All', the DNA-binding dye DAPI (4,6-diamidino-2-phenylindole) and DNase I were purchased from Sigma (Poole, Dorset, U.K.). Primary antibodies were obtained from Affinity Bioreagents [Golden, CO, U.S.A.; mAb XIIC4 to SAR, mAb IIH11 to the fast SERCA1 (sarcoplasmic/endoplasmic-reticulum Ca^{2+}-ATPase 1) isoform of the Ca^{2+}-ATPase and mAb VIIID1_2 to CSQ], Sigma (polyclonal antibody to LAM), Upstate Biotechnology [Lake Placid, NY, U.S.A.; mAb C464.6 to the α_1-subunit of the Na^+/K^+-ATPase and mAb VIA4_1 to α-DG (α-dystroglycan)] and Novacastra Laboratories [Newcastle upon Tyne, U.K.; mAb NCL-43 to β-DG (β-dystroglycan) and mAb DYS-2 to the C-terminus of the Dp427 isoform of dystrophin]. Antibodies to Up395 (utrophin of 395 kDa) and HRC were gifts from Dr S. Winder (University of Sheffield, U.K.) and Dr W. J. Park (Kwangju Institute of Science, Kwangju, Korea) respectively. Peroxidase-, rhodamine- or fluorescein-conjugated secondary antibodies were obtained from Chemicon (Temecula, CA, U.S.A.) and Superfrost Plus positively charged microscope slides were from Menzel Glässer (Braunschweig, Germany). All other chemicals used were of analytical grade and purchased from Sigma.

Dystrophic muscle specimens

The mdx mouse model of Duchenne muscular dystrophy [28] is characterized by the absence of the Dp427 isoform of the membrane cytoskeletal element dystrophin owing to a point mutation in exon 23 [29]. We obtained 6-, 8- and 24-week-old male mice of the Dmd^{mdx} strain (Jackson Laboratory, Bar Harbor, ME, U.S.A.) and age-matched controls from the Biomedical Facility of the National University of Ireland (Dublin, Ireland). To compare the expression of SAR in normal versus mdx skeletal muscles, tissue specimens were prepared for (i) detergent extraction of the total muscle protein complement to perform one- and two-dimensional immunoblot analyses, (ii) subcellular fractionation to perform immunoblotting of the SR-enriched microsomal fraction, and (iii) cryosectioning for immunofluorescence localization studies. For immunoblot analysis, skeletal-muscle samples were quick-frozen in liquid nitrogen, transferred to a container with solid CO_2 and stored at -70 °C before homogenization. For immunofluorescence microscopy, muscle specimens were carefully dissected and immediately quick-frozen in liquid nitrogen-cooled isopentane, transferred to a container with solid CO_2 and stored at -70 °C before cryosectioning.

Two-dimensional gel electrophoresis of total muscle extracts

The abundance of SAR in crude muscle extracts was determined by one-dimensional immunoblot analysis and two different two-dimensional techniques. One-dimensional immunoblot analysis and diagonal non-reducing/reducing two-dimensional gel electrophoresis were performed as described previously [30,31]. Two-dimensional electrophoresis with IEF (isoelectric focusing) in the first dimension was specifically optimized for the separation of muscle proteins. Before IEF, whole muscle sections (0.2 g wet weight) were ground to a fine powder using liquid nitrogen and subsequently solubilized in lysis buffer containing 9.5 M urea, 4 % (w/v) Chaps, 0.5 % (v/v) carrier ampholytes 3–10 and 100 mM DTT (dithiothreitol). To avoid protein degradation, the solution was supplemented with a freshly prepared protease inhibitor cocktail [0.2 mM pefabloc, 1.4 μM pepstatin, 0.15 μM aprotinin, 0.3 μM *trans*-epoxysuccinyl-L-leucylamido-(4-guanidino)butane ('E-64'), 1 μM leupeptin, 0.5 mM soyabean trypsin inhibitor and 1 mM EDTA]. To eliminate the excessive viscosity of the extract due to DNA, 2 μl of DNase I (200 units) was added per 100 μl of lysis buffer. After incubation at room temperature (20 °C) for 3 h (whereby samples were vortex-mixed every 10 min for 5 s), the suspension was centrifuged at 20 000 ***g*** for 20 min at 4 °C in an Eppendorf 5417R centrifuge (Hamburg, Germany). The supernatant was diluted in IPG-strip lysis buffer [complemented with 0.05 % (w/v) Bromophenol Blue tracking dye] to achieve a final protein concentration of 50 μg of protein/IEF strip for silver staining or immunoblotting. IEF was performed on individual 7-cm-long IPG strips at 60 μA/strip using an IPGphor IEF system obtained from Amersham Biosciences. The run conditions were as follows: a 30 V step for 12 h, 200 V for 1 h, 500 V for 1 h, 1000 V for 1 h, 2000 V for 1 h, 4000 V for 2 h and, finally, 6000 V for 6 h [32]. After IEF, the cover fluid was poured off and the strips were stored at -70 °C until further use. Before separation in the second-dimension gel system, focused strips were equilibrated for 30 min in a solution of 30 % (w/v) glycerol, 20 % (w/v) sucrose, 3 % (w/v) SDS, 6 M urea, 50 mM Tris/HCl

(pH 8.8) and 100 mM DTT, and a further 30 min equilibration was performed employing 250 mM iodoacetamide instead of 100 mM DTT. After equilibration, the strips were embedded in an agarose solution containing 0.5 % (w/v) agarose in standard SDS electrophoresis buffer [25 mM Tris/192 mM glycine, pH 8.3/0.1 % (w/v) SDS]. Second-dimension electrophoresis was performed with a 7.5 % (w/v) separation gel for 210 Vh [33]. Silver staining, immunoblotting and enhanced chemiluminescence were performed by standard methodology [30]. Densitometric scanning of enhanced chemiluminescence blots was performed on a Molecular Dynamics 300S computing densitometer (Sunnyvale, CA, U.S.A.) using ImageQuant V3.0 software. Differences between means were evaluated using an unpaired two-sided Student's t test, where $P < 0.05$ was considered to be significant. Labelling of Ca^{2+}-binding elements with the cationic carbocyanine dye 'Stains All' was performed by the method of Campbell et al. [34].

Biochemical analysis of microsomes

For immunoblotting, 'Stains All' labelling, chemical cross-linking and differential co-immunoprecipitation analysis of the SR from normal and dystrophic muscles, the microsomal fraction was isolated by an established method at 0–4 °C [35] in the presence of the protease inhibitor cocktail described above. The membranes were resuspended at a protein concentration of 10 mg/ml and then used immediately for gel electrophoretic separation and biochemical analyses. Protein concentration was determined by the method of Bradford [36], using BSA as a standard. A Mini-MP3 electrophoresis system and a mini blotting cell, obtained from Bio-Rad Laboratories (Hemel Hempstead, Herts., U.K.), were used for the one-dimensional gel electrophoretic separation of microsomal muscle proteins under reducing conditions. We used 7 % (w/v) resolving gels and 25 μg of protein/lane. Microsomal proteins were electrophoretically transferred for 1 h at 100 V on to nitrocellulose membranes. Incubation with antibodies, visualization of immunodecorated protein bands and densitometric scanning of developed immunoblots were performed as described previously in detail [30]. Chemical cross-linking of muscle-membrane proteins using the hydrophobic 1.2 nm probe, DTSP [dithiobis(succinimidyl propionate)], was performed by an established method [35]. Cross-linker-stabilized complexes, as indicated by DTSP-induced shifts to lower electrophoretic mobilities, were determined by immunoblot analysis of non-reducing gels. Immunoprecipitation experiments were performed as described by Culligan et al. [16].

Immunofluorescence microscopy

Cryosections of 12 μm thickness were prepared on a Microm cryostat (Heidelberg, Germany) and mounted on to Superfrost Plus positively charged microscope slides. After fixation and blocking [16], sections were incubated with primary antibodies, carefully washed and then incubated with fluorescein- or rhodamine-conjugated secondary antibodies. Images were obtained by an established methodology [16]. To outline the cellular periphery in cryosections labelled with antibodies to SAR, fibres were double-stained for the surface marker LAM. For double immunostaining, a mixture of the two primary antibodies was applied to the muscle sections for 1 h at 37 °C. Subsequently, cryosections were washed and then separately incubated, for 30 min each, with a differently conjugated secondary antibody. Internal SAR staining with a fluorescein probe and LAM labelling with a rhodamine-conjugated antibody were performed. For labelling the position of nuclei within fibres, cryosections were incubated with the DNA-binding dye DAPI [18].

RESULTS

Reduced expression of SAR in mdx skeletal muscles

On the basis of recent findings that luminal Ca^{2+} sequestration is significantly reduced in dystrophin-deficient fibres [16] and that the oligomerization of the terminal cisternae Ca^{2+}-binding protein, CSQ, is impaired in mdx skeletal muscles [18], the present study investigated potential changes in another abundant luminal SR Ca^{2+}-binding element, namely the 160 kDa protein SAR [17]. Although certain biochemical analyses of relatively low-abundance proteins can be performed properly only with enriched vesicular preparations, it cannot be excluded that extensive subcellular fractionation procedures may introduce artifacts. Therefore, before performing a more detailed immunoblotting survey, chemical cross-linking studies and differential co-immunoprecipitation experiments of microsomal membranes, we first analysed the total muscle protein complement by one- and two-dimensional electrophoresis. As shown in Figure 1, the expression of SAR is significantly reduced in dystrophic mdx muscles when compared with age-matched control specimens. In contrast with relatively comparable levels of the Na^+/K^+-ATPase (Figures 1A and 1C) and 53-SRGP (Figures 1B and 1E), immunodecoration of the 160 kDa SAR band revealed an approx. 70 % decrease in density in mdx muscle (Figures 1B and 1D). Immunoblotting of nitrocellulose replicas after diagonal non-reducing/reducing two-dimensional gel electrophoresis agreed with results from the one-dimensional analysis. The intensity of the SAR band was greatly decreased in the mdx protein complement when compared with normal controls (Figures 1F and 1G). The protein band representing SAR formed a vertical immunolabel, indicative of a heterogeneous mixture of protein species after chemical reduction. This has been described previously for other microsomal proteins, such as the α_2-subunit of the transverse-tubular dihydropyridine receptor [32].

Standard two-dimensional gel electrophoresis using IEF in the first dimension and SDS/PAGE in the second dimension confirmed the drastic reduction of SAR in mdx muscles. Although the overall silver-stained spot pattern was found to be relatively comparable between the normal and dystrophic protein complement, individual protein spots exhibited a different intensity (Figures 2A and 2B). Therefore this result seemed to be compatible with a proteomics-based approach towards identifying specific proteins by digesting spots with trypsin, followed by MS. Although our laboratory previously applied MS successfully to identify digested fragments of microsomal muscle isoforms [37], this approach failed in the analysis of crude muscle extracts owing to the high background levels of myofibrillar elements (results not shown). In muscles, approximately half the protein complement is represented by myosin, actin, troponin and tropomyosin. Fragments of these abundant proteins prevent a proper MS identification of the muscle Ca^{2+}-binding proteins of interest. Therefore databanks of standardized two-dimensional gels, such as the ExPASy SWISS-2DPAGE mouse tissue library, only list abundant proteins [38]. Although it was not possible to identify a specific protein spot corresponding to SAR using MS, immunoblotting with mAb C464.6 to the α_1-subunit of the Na^+/K^+-ATPase and mAb XIIC4 to SAR recognized their respective antigens after two-dimensional gel electrophoresis. In contrast with comparable levels of the α_1-Na^+/K^+-ATPase in normal and mdx muscles (Figures 2C, 2D and 2G), SAR expression

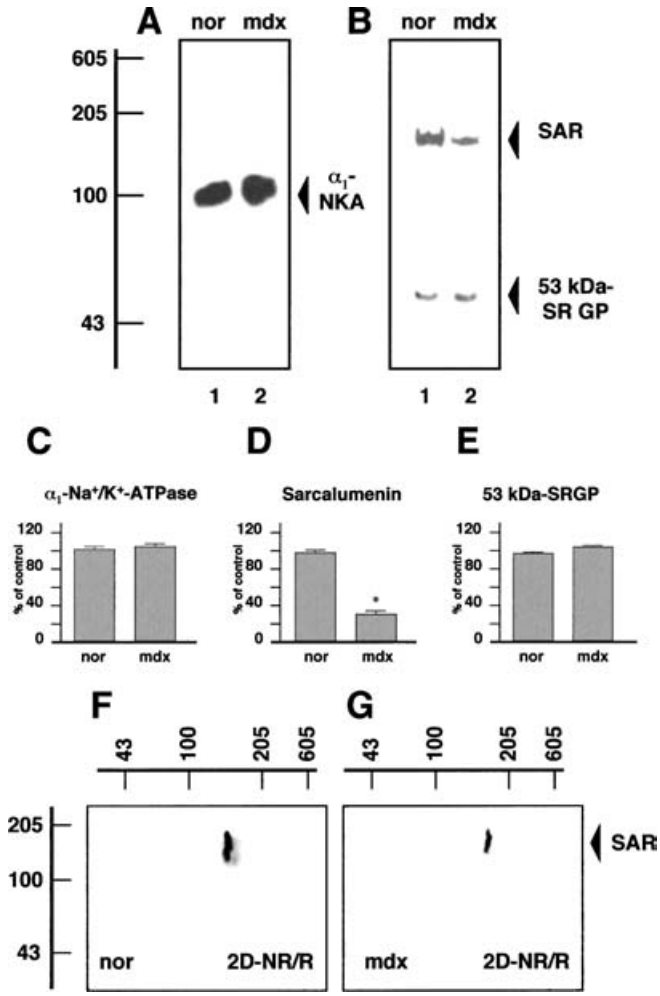

Figure 1 Immunoblot analysis of SAR expression in crude muscle extracts

(**A**, **B**) Immunoblots of total extracts from normal (lane 1, nor) and dystrophic mdx (lane 2) skeletal muscles, labelled with antibodies to α_1-Na^+/K^+-ATPase (α_1-NKA) (**A**), as well as SAR (**B**) and 53-SRGP (**B**). Molecular-mass standards (in kDa) are indicated on the left. (**C**–**E**) Graphical representation of the immunoblot analysis ($n = 5$; $^*P < 0.05$, unpaired t test). (**F**, **G**) Immunoblot analyses of SAR in normal and dystrophic muscles respectively after diagonal non-reducing/reducing two-dimensional gel electrophoresis (2D-NR/R). Molecular-mass standards (in kDa) are indicated on the left and on the top of blots. Positions of immunodecorated proteins are marked by the arrowhead.

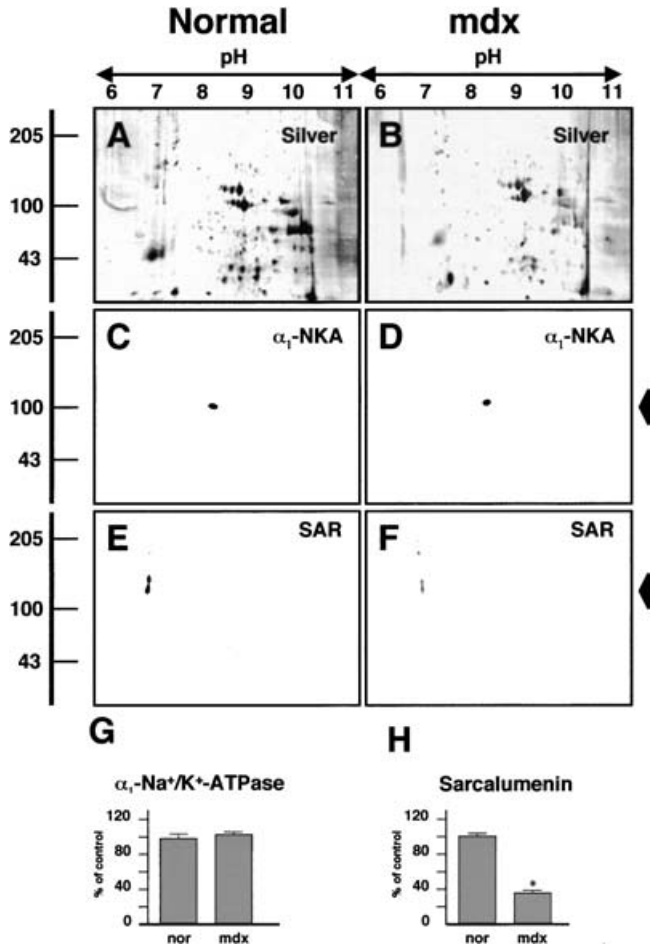

Figure 2 Comparative two-dimensional immunoblot analysis of SAR expression in normal and mdx muscle extracts

Silver-stained gels (**A**, **B**) and the corresponding immunoblots (**C**–**F**) of total extracts from normal (**A**, **C**, **E**) and dystrophic mdx (**B**, **D**, **F**) skeletal muscles. Immunoblots were labelled with antibodies to α_1-NKA (**C**, **D**) and SAR (**E**, **F**). The relative position of immunodecorated dots representing SAR and Na^+/K^+-ATPase are marked by arrowheads. The pH values of the first dimension gel system and molecular-mass standards (in kDa) of the second dimension are indicated on the top and on the left of the panels respectively. (**G**, **H**) Graphical representation of the immunoblot analysis ($n = 5$; $^*P < 0.05$, unpaired t test).

was found to be significantly reduced in Dp427-deficient muscles (Figures 2E, 2F and 2H).

Reduced expression of SAR in mdx SR

Before chemical cross-linking and immunoprecipitation analysis of mdx microsomes, expression levels of membrane markers were determined in the SR-enriched subcellular fraction. The mutant status of the mdx preparation was confirmed by the complete absence of the dystrophin band of 427 kDa apparent mass (Figures 3A and 3F). An antibody to the autosomal homologue of Dp427, the 395 kDa dystrophin-related protein named utrophin [39], revealed a comparable density of Up395 in normal and mdx membranes (Figure 3B). As described previously, dystrophin-associated glycoproteins, such as β-DG, were shown to be greatly reduced in Dp427-deficient membranes (Figures 3C and 3G). No marked differences in the expression of the fast SERCA1 isoform of the SR Ca^{2+}-ATPase (Figures 3D and 3H) were detectable by immunoblotting. Immunolabelling of the luminal SR Ca^{2+}-binding protein HRC [40] revealed no alteration in its relative density in muscular dystrophy (Figure 3E).

Incubation of electrophoretically separated proteins with the cationic carbocyanine dye named 'Stains All' specifically labels major Ca^{2+}-binding elements with a characteristic blue colour [34], whereas other protein bands are stained in pink. As illustrated in Figure 4(A), the 'Stains All' dye labelled a major microsomal band at 63 kDa apparent mass and three minor bands in the 150–220 kDa range. Figure 4(A) (lane 3) diagrammatically outlines this staining pattern whereby the 63 kDa band corresponds to the CSQ monomer. The upper three bands having lower electrophoretic mobility represent overlapping bands consisting of CLP-150, CLP-170, SAR, HRC and CLP-220. Whereas 'Stains All' labelling is a relatively crude labelling method, immunoblotting using mAbs is a much more sensitive and specific technique. This might explain why the 'Stains All' panel did

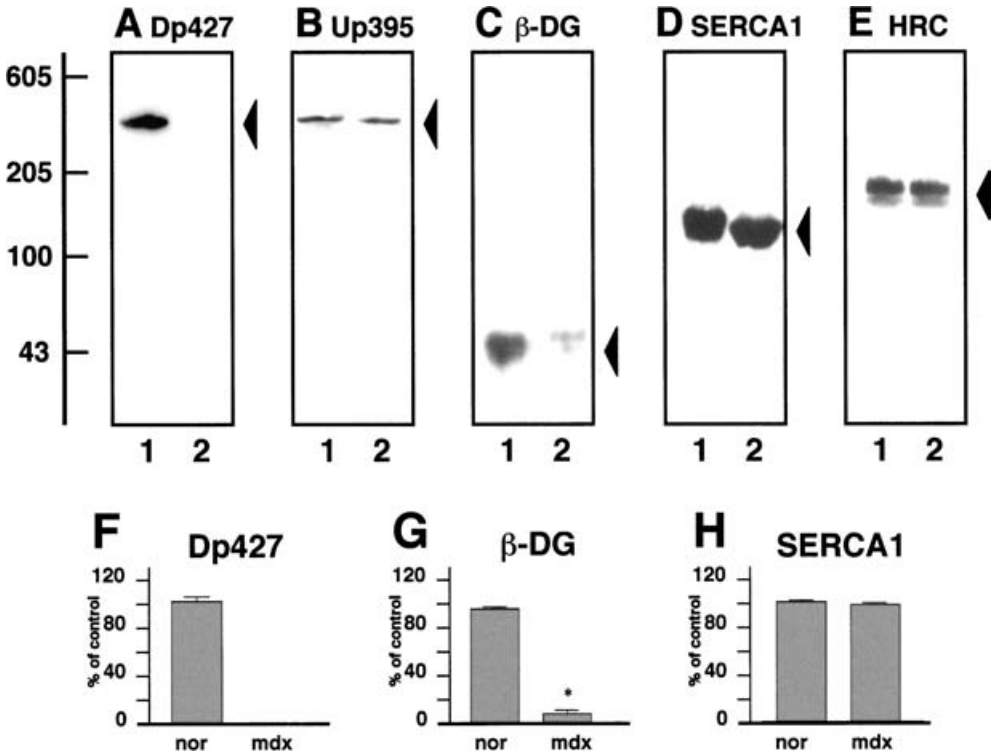

Figure 3 Characterization of the microsomal fraction from normal and mdx skeletal muscles

(**A**–**E**) Immunoblots of microsomal membranes from normal (lane 1, nor) and dystrophic mdx (lane 2) skeletal muscles, labelled with antibodies to the Dp427 isoform of dystrophin (**A**), the Up395 isoform of utrophin (**B**), the dystrophin-associated glycoprotein β-DG (**C**), the fast SERCA1 isoform of the SR Ca^{2+}-ATPase (**D**) and HRC (**E**). Molecular-mass standards (in kDa) are indicated on the left. The position of immunodecorated proteins are marked by arrowheads. (**F**–**H**) Graphical representation of the immunoblot analysis ($n = 5$; $^*P < 0.05$, unpaired t test).

not exhibit major differences in the expression pattern of Ca^{2+}-sequestrating proteins (Figure 4A), whereas the immunoblot analysis of microsomal membranes clearly revealed a significant reduction in CLPs (Figures 4B and 4D). The fast CSQ monomer of 63 kDa apparent mass was shown to be not affected in mdx membranes (Figures 4B and 4C).

Figure 5 illustrates the immunoblot analysis of 6-, 8- and 24-week-old mdx fibres. SAR expression was clearly reduced in all the age groups studied (Figures 5A and 5C). Since immunoblotting of younger specimens did not result in proper staining patterns above background (results not shown), we could not evaluate younger mdx fibres. This is due to the difficulty in performing proper subcellular fractionation studies using small sample sizes of developing mouse muscles and the relatively low density of SAR in total tissue extracts. In contrast with decreased SAR levels in older mdx fibres, the expression of the surface α_1-Na^+/K^+-ATPase was not changed in 6–24-week-old mdx specimens (Figures 5B and 5D). Therefore both the Na^+/K^+-ATPase and CSQ can be employed for convenient internal standardization of immunoblots. This demonstrates that the reduction in SAR and CLPs is not an artifact of the subcellular fractionation technique, gel electrophoresis, transfer to nitrocellulose, immunodecoration and/or the enhanced chemiluminescence detection method.

Complex formation between SAR and Ca^{2+}-ATPase

Electron microscopical localization studies by Leberer et al. [19] suggest a close neighbourhood relationship between SAR and the SR Ca^{2+}-ATPase. To evaluate whether these two SR proteins exist in a tight complex as judged by biochemical criteria and to determine whether the protein–protein interactions are disturbed in the dystrophic phenotype, chemical cross-linking and differential co-immunoprecipitation were performed.

Increasing concentrations of the hydrophobic probe DTSP induced a shift of the SERCA1 band to a position with a drastically reduced electrophoretic mobility (Figure 6A). In analogy, cross-linker-stabilized oligomerization was also observed for SAR (Figure 6B). A decrease in the monomeric bands of SAR and SERCA1, as well as an increase in the oligomeric conformation, was detected both in normal and mdx membranes. Although the expression of SAR is drastically reduced in mdx microsomes, the mass of the DTSP-stabilized oligomeric species appears to be identical in normal and mdx muscles (Figure 6B). The fact that the high-molecular-mass bands of both SR proteins exhibited a potential overlap after cross-linking indicates the existence of a supramolecular complex between SAR and SERCA1. However, since the electrophoretic behaviours of protein assemblies with very high molecular mass do not exhibit a linear relationship, the overlap between both the DTSP-induced bands may be coincidental.

Hence, to validate the findings from the cross-linking analysis, differential co-immunoprecipitation was performed. Before studying the potential complex between SAR and SERCA1, it was examined whether this technique was capable of determining not only protein–protein interactions, but also the relative reduction in individual components owing to muscular dystrophy. As shown in Figures 7(A) and 7(B), an antibody to LAM precipitated its own antigen and another member of the dystrophin–glycoprotein complex α-DG. The fact that α-DG is greatly reduced in mdx

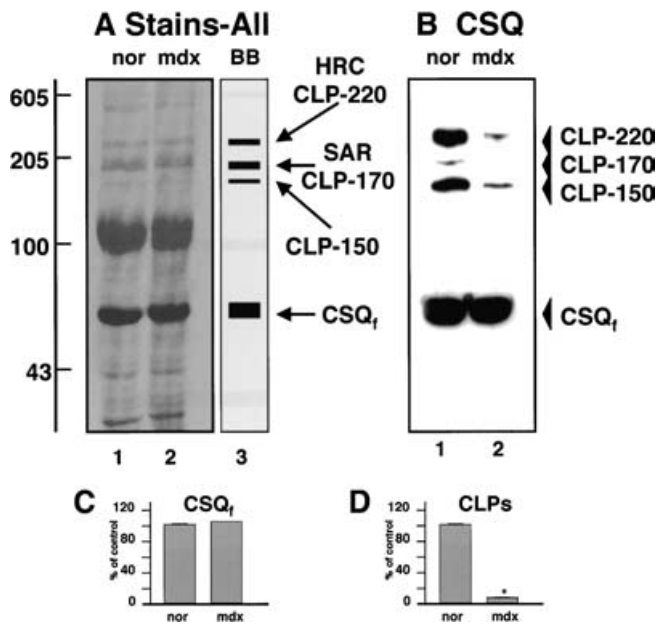

Figure 4 Reduced expression of CLPs in mdx microsomal fraction

A 'Stains All'-labelled gel (**A**) and the corresponding immunoblot of microsomes from normal (lane 1, nor) and dystrophic mdx (lane 2) skeletal muscles, labelled with an antibody to CSQ (CSQ_f) and the CSQ-like proteins CLP-150, CLP-170 and CLP-220 (**B**). In (**A**), lane 3 is a diagrammatic presentation of blue bands (BB) stained with the cationic carbocyanine dye 'Stains All'. The 'Stains All'-labelled band of 63 kDa apparent mass is the CSQ monomer and the high-molecular-mass bands represent CLP-220 and HRC at approx. 220 kDa, CLP-170 and SAR at approx. 170 kDa and CLP-150 at approx. 150 kDa. Molecular-mass standards (in kDa) are indicated on the left. Positions of immunodecorated proteins are marked by arrowheads. (**C**, **D**) Graphical representation of the immunoblot analysis ($n = 5$; $^*P < 0.05$, unpaired t test).

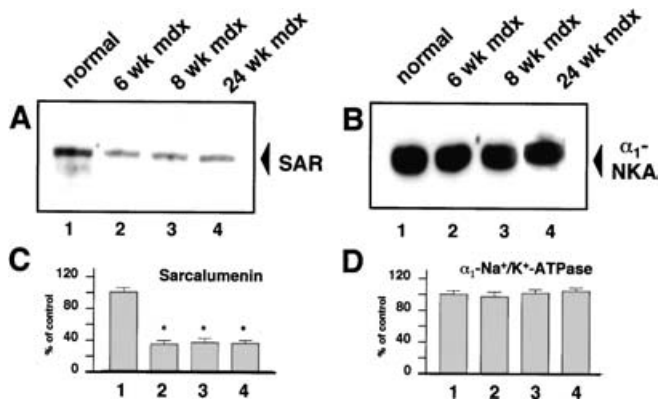

Figure 5 Reduced expression of SAR in mdx microsomal fraction

(**A**, **B**) Immunoblots of microsomes from normal (lane 1, nor) and 6-week-old (lane 2), 8-week-old (lane 3) and 24-week-old (lane 4) dystrophic mdx skeletal muscles, labelled with antibodies to SAR (**A**) and α_1-NKA (**B**). Positions of immunodecorated proteins are marked by arrowheads. (**C**, **D**) Graphical representation of the immunoblot analysis ($n = 5$; $^*P < 0.05$, unpaired t test).

fibres but LAM is not markedly changed [7] is clearly reflected by the immunoprecipitation results. In quantitative terms, results from comparative immunoprecipitation experiments are not as reliable as immunoblotting owing to potential variations in the interactions between antigens and antibodies in different starting materials. However, this method is widely employed in a semi-quantitative approach. Using antibodies to SAR or

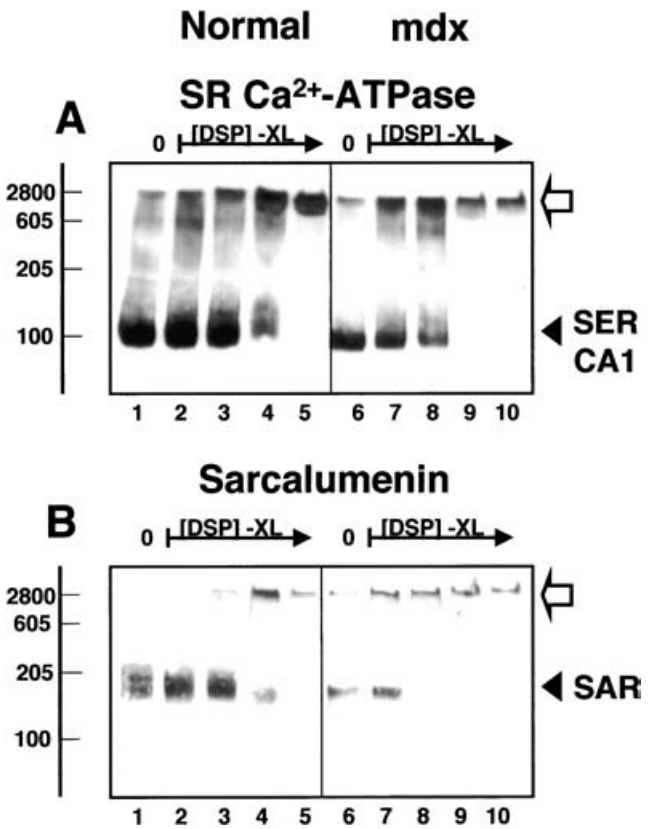

Figure 6 Chemical cross-linking analysis of SAR and Ca^{2+}-ATPase in normal and mdx microsomes

Immunoblots labelled with antibodies to the fast SERCA1 isoform of the SR Ca^{2+}-ATPase (**A**) and SAR (**B**) are shown. Lanes 1–5 (normal) and lanes 6–10 (mdx) represent 0, 25, 50, 200 and 500 μg of DTSP cross-linker (XL) per mg of microsomal membrane protein respectively. Positions of immunodecorated monomers are indicated by arrowheads and DTSP-stabilized oligomeric bands by open arrows. Molecular-mass standards (in kDa) are indicated on the left.

SERCA1, both their own antigen and the respective binding partner were precipitated (Figures 7C–7F). This finding supports the results from the cross-linking study. Furthermore, in mdx membranes, both antibodies bound considerably less SAR when compared with normal membranes (Figures 7C and 7F). This result agrees with the reduced expression of SAR in mdx muscle as shown above by one- and two-dimensional immunoblot analyses (Figures 1, 2 and 5).

Decreased SAR levels in dystrophin-deficient muscle fibres

To investigate the expression of SAR on the single fibre level, we performed indirect immunofluorescence microscopy. The labelling of transverse cryosections with an antibody to the Dp427 isoform of dystrophin confirmed peripheral localization of this membrane cytoskeletal element in normal muscle (Figure 8A) and the mutant status of mdx fibres (Figure 8B). Blue DAPI staining showed the peripheral position of nuclei in normal fibres (Figures 8A and 8C) and the drastic increase in centrally located myonuclei in dystrophin-deficient cells (Figures 8B and 8D). For internal standardization of immunolabelling and to outline the cellular periphery, tissue sections were co-incubated with antibodies to LAM. In contrast with the relatively comparable Rhodamine staining of LAM in the cell-surface structure, green

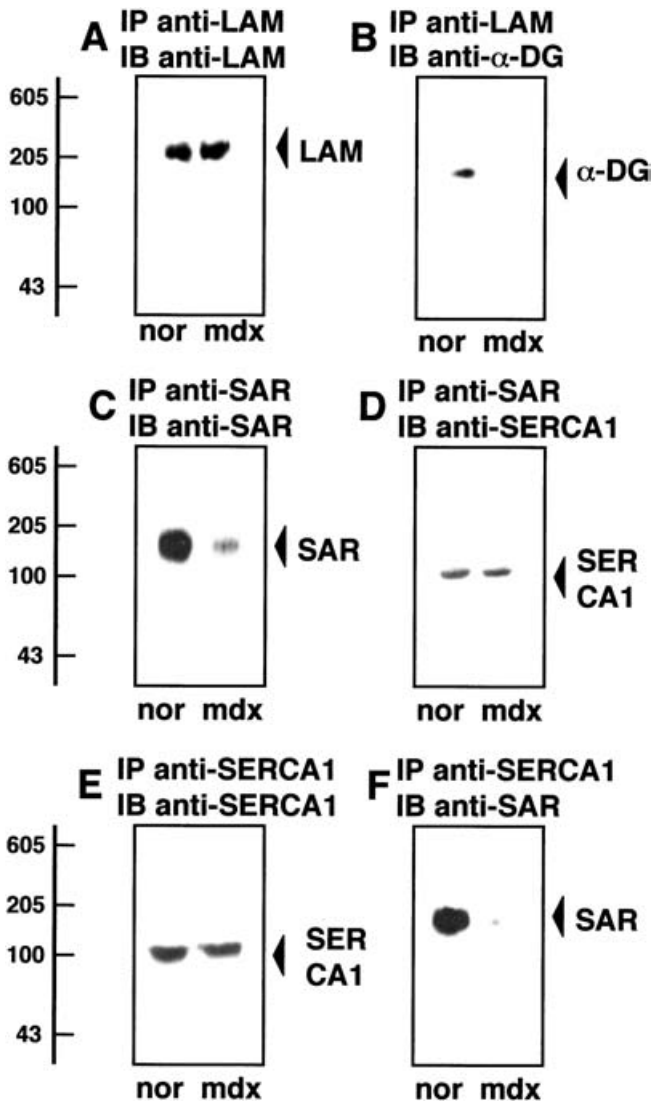

Figure 7 Differential co-immunoprecipitation analysis of SAR and Ca^{2+}-ATPase in normal and mdx microsomes

Immunoblots of solubilized microsomes immunoprecipitated (IP) with antibodies to LAM (**A**, **B**), SAR (**C**, **D**) and the fast SERCA1 isoform of the SR Ca^{2+}-ATPase (**E**, **F**). Immunoblots (IB) were labelled with antibodies to LAM (**A**), α-DG (**B**), SAR (**C**, **F**) and the SR Ca^{2+}-ATPase (**D**, **E**). Lanes 1 and 2, microsomal membranes isolated from normal control and dystrophic mdx skeletal muscles respectively. Positions of immunodecorated proteins are marked by arrowheads. Molecular-mass standards (in kDa) are indicated on the left.

fluorescein labelling of SAR was found to be greatly reduced in mdx fibres (Figures 8C and 8D). The regular punctuated staining pattern of SAR in the interior of normal fibres, representative of its luminal SR localization, is not present in mdx muscles. Instead, more patchy immunodecoration is visible in mdx fibres (Figure 8D).

Therefore the results of our analysis of SAR expression using one-dimensional immunoblotting of crude muscle extracts (Figure 1), two-dimensional immunoblotting of crude muscle extracts (Figure 2), immunoblotting of microsomes (Figure 5), immunoprecipitation (Figure 7) and immunofluorescence microscopy (Figure 8) agree with each other and they demonstrate drastically decreased levels of this luminal SR Ca^{2+}-binding protein in muscular dystrophy.

DISCUSSION

Duchenne muscular dystrophy represents the most frequent gender-specific disease of childhood [41]. Although the primary abnormality was elucidated 17 years ago [42] and has certainly led to a greatly improved diagnosis of muscular disorders [43], this biomedical knowledge has not yet improved the quality of life or life expectancy of dystrophic children. It is not known how the absence of dystrophin leads to muscle weakness. Knowing the general symptoms of end-stage pathology and having elucidated the specific genetic defect in a neuromuscular disorder does not necessarily lead to a comprehensive molecular and cellular understanding of a muscle disease process. Clinical information regarding the onset, progression and severity of symptoms, the symmetry of muscular weakness, the involvement of other organs and the patient's family history is often of limited help in the identification of the secondary pathophysiological pathways leading to muscle degradation. Histopathological findings such as abnormal variation in fibre diameter, rounded muscle cells, central nucleation, the occurrence of necrotic and regenerating cells and the infiltration of connective and fatty tissues usually do not explain the molecular mechanisms underlying contractile weakness. Thus, in addition to the genetic analysis of muscle diseases, it is crucial to perform comprehensive pathobiochemical analyses of diseased muscle specimens to identify secondary defects, which may be exploited in future approaches to counteract symptoms of muscular disorders [26,27].

Although the mdx mouse does not exhibit all symptoms of severe human Duchenne muscular dystrophy, it is a well-established model of the X-chromosome-linked muscle disease and is widely employed in biomedical research [44]. In the present study, we have analysed Dp427-deficient mdx skeletal-muscle fibres and could demonstrate that expression of the luminal SR Ca^{2+}-binding protein SAR of 160 kDa apparent mass is drastically reduced in muscular dystrophy and its SR domains appear to be changed in Dp427-deficient fibres. SAR has been postulated to function as an intraluminal ion transporter, in addition to its physiological role as a Ca^{2+}-buffering element [19]. The regular punctuated staining pattern of SAR in the interior of the normal fibre probably reflects its luminal SR localization. In stark contrast, the patchy immunofluorescence labelling of mdx fibres indicates a potential re-organization of SAR domains within the complex SR membrane system. In contrast, CSQ domains are not affected in mdx muscles [16]. This suggests that impaired Ca^{2+} buffering within the mdx SR is caused by both reduced SAR expression and impaired CSQ oligomerization [16,18]. Perhaps more importantly, the abnormal domain formation of SAR indicates an impaired Ca^{2+} shuttling between the Ca^{2+}-uptake SERCA units and the major terminal cisternae Ca^{2+}-binding CSQ clusters via SAR. This finding might be of potential importance for explaining the observed Ca^{2+}-induced myonecrosis in muscular dystrophy [45].

As shown in Scheme 1, the increase in sarcolemmal Ca^{2+}-leak channel expression after exercise-induced membrane rupturing and natural membrane re-sealing appears to be the main factor for the increase in cytosolic Ca^{2+} levels [11]. To what extent the perturbation of Ca^{2+} homoeostasis affects all cytosolic domains in end-stage muscular dystrophy is debatable. Most probably, the cytosolic Ca^{2+} overload in Dp427-deficient muscle cells is not of a global nature, but is restricted to the subsarcolemmal domain [10]. Skeletal-muscle membranes that exhibit a greatly reduced dystrophin–glycoprotein complex lose their sarcolemmal integrity. This in turn causes a dramatic increase in exercise-induced membrane rupturing [8]. During the natural processes of cell-membrane resealing, these transient microruptures

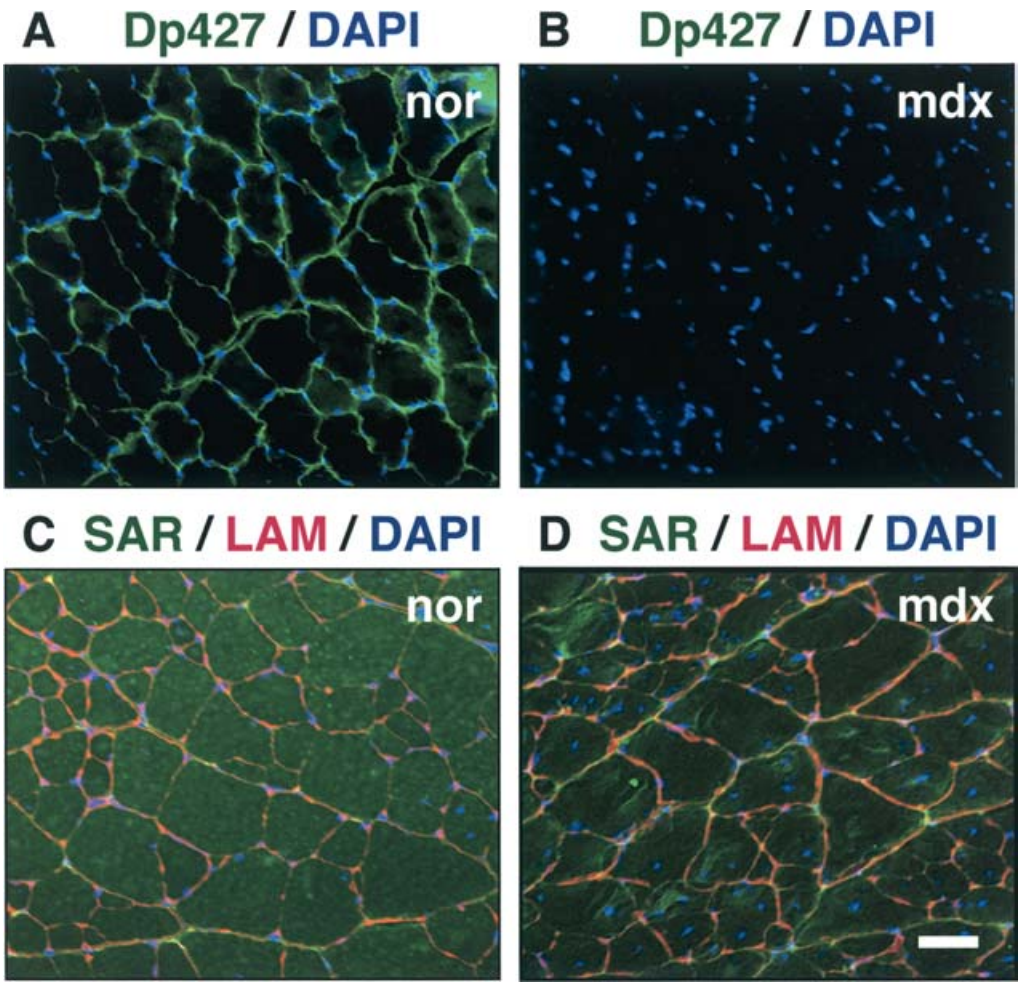

Figure 8 Immunofluorescence localization of SAR in mdx muscles

Cryosections labelled with antibodies to the Dp427 isoform of dystrophin (green) (**A**, **B**), SAR (green) (**C**, **D**) and LAM (red) (**C**, **D**). Nuclei were stained with the DNA-binding dye DAPI (blue) (**A**–**D**). Skeletal-muscle specimens were taken from normal (**A**, **C**) and mdx (**B**, **D**) skeletal-muscle fibres. Sarcolemmal dystrophin staining was absent from mdx fibres. LAM staining was almost exclusively found in the cellular periphery, and the punctuated labelling of SAR occurred mostly in the internal structures of normal fibres. In dystrophic muscles, immunodecoration of SAR showed an overall reduction and a more patchy pattern. Scale bar, 40 μm.

allow for the insertion of Ca^{2+}-leak channels into the dystrophic sarcolemma. Localized increases in Ca^{2+} contribute a pathophysiological cycle of enhanced protease activity and Ca^{2+}-channel activation. This phenomenon is exacerbated by abnormal Ca^{2+} cycling through the SR lumen [16] and possibly also the mitochondria [46]. Impaired CSQ clustering [18] and reduced SAR expression, as described in the present study, may both contribute to decreased luminal Ca^{2+} buffering. The muscular degeneration process might be amplified by increased free cytosolic Ca^{2+} levels. Consequently, increased sarcolemmal Ca^{2+} fluxes seem to influence indirectly luminal SR Ca^{2+} cycling, which is probably a major factor in the progressive functional decrease in Dp427-deficient muscle cells. In this respect, our study clearly supports the calcium hypothesis of muscular dystrophy [10–13,16].

One of the most promising new ways of determining global changes in diseases is biomedical proteome research using high-resolution two-dimensional electrophoresis and MS for the identification of abnormal protein expression patterns [47]. However, this approach does not cover many low-abundance proteins, hydrophobic membrane elements, very basic components and exceptionally large proteins involved in muscle pathology [48]. Therefore the conventional identification of electrophoretically separated muscle proteins using one- or two-dimensional immunoblot analyses, as presented here, still represents a powerful tool for the initial identification of the secondary abnormalities leading to fibre destruction. For mdx, muscle proteomics (using standard two-dimensional electrophoresis of total muscle extracts) would not have led to the initial identification of dystrophin as a primary abnormality for two reasons: (i) the full-length skeletal-muscle isoform of dystrophin has an apparent molecular mass of 427 kDa and therefore does not properly transfer from the first-dimension IEF gel to the second-dimension slab gel, and (ii) the Dp427 isoform of the membrane cytoskeleton is a relatively low-abundance protein and does not show up as a distinct protein spot on two-dimensional gels. On the other hand, comparative subcellular fractionation studies, using lectin agglutination methods for the affinity isolation of muscle sarcolemma vesicles, clearly revealed the absence of dystrophin from dystrophic surface membrane preparations

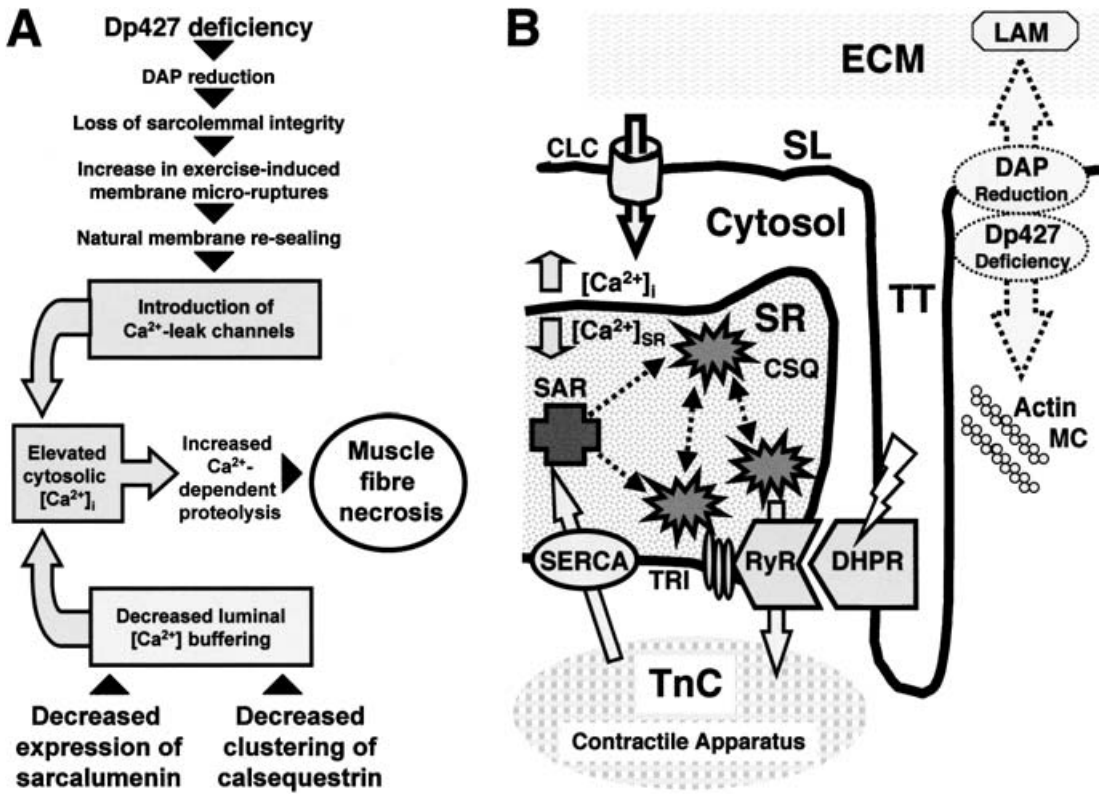

Scheme 1 Overview of the calcium hypothesis of muscular dystrophy

The flow chart (**A**) and the diagram (**B**) integrate the findings of our analysis of SAR expression in dystrophin-deficient skeletal-muscle fibres into the well-established calcium hypothesis of muscular dystrophy. Absence of the Dp427 isoform of dystrophin triggers a drastic reduction in dystrophin-associated proteins (DAP). Loss of the linkage between the actin membrane cytoskeleton (MC) and the extracellular matrix (ECM) protein LAM results in increased exercise-induced membrane microrupturing. Subsequently, Ca^{2+}-leak channels are introduced into the sarcolemma (SL) after membrane resealing, which in turn triggers the influx of Ca^{2+} ions into the cytosol. This pathophysiological effect is exacerbated by an impaired Ca^{2+}-buffering capacity of the SR. Both decreased CSQ clustering and reduced expression of SAR, as shown in the present study, cause abnormal Ca^{2+} cycling through the lumen of the SR (**A**). The resulting increased cytosolic Ca^{2+} levels then trigger Ca^{2+}-induced proteolysis, which eventually leads to severe muscular weakness. (**B**) The complex interaction between various Ca^{2+}-regulatory proteins and how disturbances in the luminal Ca^{2+}-cycling process may trigger impaired excitation–contraction coupling are shown. Direct physical coupling between the voltage-sensing dihydropyridine receptor (DHPR) of the transverse tubules (TT) and the ryanodine receptor (RyR) of the junctional SR causes Ca^{2+} release into the cytosol and thereby troponin C (TnC)-mediated muscular contraction. Interactions between the RyR and CSQ clusters are maintained by triadin (TRI). The energy-dependent re-uptake of Ca^{2+} ions into the SR lumen via the SERCA Ca^{2+} pumps triggers muscle relaxation. The luminal Ca^{2+}-binding element SAR is postulated to act as an ion shuttle between the Ca^{2+}-pump units and the Ca^{2+}-reservoir complex of the terminal cisternae, which consists mostly of CSQ clusters. In conjunction with the overexpression of Ca^{2+}-leak channels (CLC) in the dystrophic sarcolemma, decreased SAR levels and impaired CSQ aggregation may play a major role in abnormal Ca^{2+} homoeostasis in muscular dystrophy.

[49]. This illustrates that conventional biochemical strategies analysing subproteomes can be successfully employed in muscle pathology and used to complement large-scale and high-throughput proteome projects.

This work was supported by project grants from Enterprise Ireland (SC/2000/386), Muscular Dystrophy Ireland (MDI-02) and the European Commission (HPRN-CT-2002-00331). We thank Dr S. Winder and Dr W. J. Park for their gifts of antibodies.

REFERENCES

1 Berridge, M. J., Bootman, M. D. and Roderick, H. L. (2003) Calcium signalling: dynamics, homeostasis and remodelling. Nat. Rev. Mol. Cell Biol. **4**, 517–529
2 Berchtold, M. W., Brinkmeier, H. and Muntener, M. (2000) Calcium ion in skeletal muscle: its crucial role for muscle function, plasticity, and disease. Physiol. Rev. **80**, 1215–1265
3 Melzer, W., Herrmann-Frank, A. and Lüttgau, H. C. (1995) The role of Ca^{2+} ions in excitation–contraction coupling of skeletal muscle fibres. Biochim. Biophys. Acta **1241**, 59–116
4 Blake, D. J., Weir, A., Newey, S. E. and Davies, K. E. (2002) Function and genetics of dystrophin and dystrophin-related proteins in muscle. Physiol. Rev. **82**, 291–329
5 Alderton, J. M. and Steinhardt, R. A. (2000) How calcium influx through calcium leak channels is responsible for the elevated levels of calcium-dependent proteolysis in dystrophic myotubes. Trends Cardiovasc. Med. **10**, 268–272
6 Campbell, K. P. (1995) Three muscular dystrophies: loss of cytoskeleton–extracellular matrix linkage. Cell (Cambridge, Mass.) **80**, 675–679
7 Ohlendieck, K. (1996) Towards an understanding of the dystrophin–glycoprotein complex: linkage between the extracellular matrix and the subsarcolemmal membrane cytoskeleton. Eur. J. Cell Biol. **69**, 1–10
8 Clarke, M. S., Khakee, R. and McNeil, P. L. (1993) Loss of cytoplasmic basic fibroblast growth factor from physiologically wounded myofibers of normal and dystrophic muscle. J. Cell Sci. **106**, 121–133
9 Squire, S., Raymackers, J. M., Vandebrouck, C., Potter, A., Tinsley, J., Fisher, R., Gillis, J. M. and Davies, K. E. (2002) Prevention of pathology in mdx mice by expression of utrophin: analysis using an inducible transgenic expression system. Hum. Mol. Genet. **11**, 3333–3344
10 Mallouk, N., Jacquemond, V. and Allard, B. (2000) Elevated subsarcolemmal Ca^{2+} in mdx mouse skeletal muscle fibres detected with Ca^{2+}-activated K^+ channels. Proc. Natl. Acad. Sci. U.S.A. **97**, 4950–4955
11 Alderton, J. M. and Steinhardt, R. A. (2000) Calcium influx through calcium leak channels is responsible for the elevated levels of calcium-dependent proteolysis in dystrophic myotubes. J. Biol. Chem. **275**, 9452–9460
12 Iwata, Y., Katanosaka, Y., Arai, Y., Komamura, K., Miyatake, K. and Shigekawa, M. (2003) A novel mechanism of myocyte degeneration involving the Ca^{2+}-permeable growth factor-regulated channel. J. Cell Biol. **161**, 957–967
13 Vandebrouck, C., Martin, D., Colson-Van Schoor, M., Debaix, H. and Gailly, P. (2002) Involvement of TRPC in the abnormal calcium influx observed in dystrophic (mdx) mouse skeletal muscle fibers. J. Cell Biol. **158**, 1089–1096

14 Collet, C., Csernoch, L. and Jacquemond, V. (2003) Intramembrane charge movement and L-type calcium current in skeletal muscle fibers isolated from control and mdx mice. Biophys. J. **84**, 251–265
15 Mulvey, C. and Ohlendieck, K. (2003) Use of continuous-elution gel electrophoresis as a preparative tool for blot overlay analysis. Anal. Biochem. **319**, 122–130
16 Culligan, K., Banville, N., Dowling, P. and Ohlendieck, K. (2002) Drastic reduction of calsequestrin-like proteins and impaired calcium binding in dystrophic mdx muscle. J. Appl. Physiol. **92**, 435–445
17 Leberer, E., Charuk, J. H., Green, N. M. and MacLennan, D. H. (1989) Molecular cloning and expression of cDNA encoding a lumenal calcium binding glycoprotein from sarcoplasmic reticulum. Proc. Natl. Acad. Sci. U.S.A. **86**, 6047–6051
18 Dowling, P., Lohan, J. and Ohlendieck, K. (2003) Comparative analysis of Dp427-deficient mdx tissues shows that the milder dystrophic phenotype of extraocular and toe muscle fibres is associated with a persistent expression of β-dystroglycan. Eur. J. Cell Biol. **82**, 222–230
19 Leberer, E., Timms, B. G., Campbell, K. P. and MacLennan, D. H. (1990) Purification, calcium binding properties, and ultrastructural localization of the 53 000- and 160 000 (sarcalumenin)-dalton glycoproteins of the sarcoplasmic reticulum. J. Biol. Chem. **265**, 10118–10124
20 Ohlendieck, K., Briggs, F. N., Lee, K. F., Wechsler, A. W. and Campbell, K. P. (1991) Analysis of excitation–contraction-coupling components in chronically stimulated canine skeletal muscle. Eur. J. Biochem. **202**, 739–747
21 Ohlendieck, K., Fromming, G. R., Murray, B. E., Maguire, P. B., Leisner, E., Traub, I. and Pette, D. (1999) Effects of chronic low-frequency stimulation on Ca^{2+}-regulatory membrane proteins in rabbit fast muscle. Pflugers Arch. **438**, 700–708
22 Kutchai, H. and Campbell, K. P. (1989) Calcium transport by sarcoplasmic reticulum of skeletal muscle is inhibited by antibodies against the 53-kilodalton glycoprotein of the sarcoplasmic reticulum membrane. Biochemistry **28**, 4830–4839
23 Shoshan-Barmatz, V., Orr, I., Weil, S., Meyer, H., Varsanyi, M. and Heilmeyer, L. M. (1996) The identification of the phosphorylated 150/160-kDa proteins of sarcoplasmic reticulum, their kinase and their association with the ryanodine receptor. Biochim. Biophys. Acta **1283**, 89–100
24 Shoshan-Barmatz, V. and Ashley, R. H. (1998) The structure, function, and cellular regulation of ryanodine-sensitive Ca^{2+} release channels. Int. Rev. Cytol. **183**, 185–270
25 Ohkura, M., Furukawa, K., Fujimori, H., Kuruma, A., Kawano, S., Hiraoka, M., Kuniyasu, A., Nakayama, H. and Ohizumi, Y. (1998) Dual regulation of the skeletal muscle ryanodine receptor by triadin and calsequestrin. Biochemistry **37**, 12987–12993
26 Badalamente, W. A. and Stracher, A. (2000) Delay of muscle degeneration and necrosis in mdx mice by calpain inhibition. Muscle Nerve **23**, 106–111
27 Spencer, M. J. and Mellgren, R. L. (2002) Overexpression of a calpastatin transgene in mdx muscle reduces dystrophic pathology. Hum. Mol. Genet. **11**, 2645–2655
28 Bulfield, G., Silver, W. G., Wight, P. A. L. and Moore, K. J. (1984) X-chromosome-linked muscular dystrophy (mdx) in the mouse. Proc. Natl. Acad. Sci. U.S.A. **81**, 1189–1192
29 Sicinski, P., Geng, Y., Ryder-Cook, A. S., Barnard, E. A., Darlison, M. G. and Barnard, P. J. (1989) The molecular basis of muscular dystrophy in the mdx mouse: a point mutation. Science **244**, 1578–1580
30 Harmon, S., Froemming, G. R., Leisner, E., Pette, D. and Ohlendieck, K. (2001) Low-frequency stimulation of fast muscle affects the abundance of Ca^{2+}-ATPase but not its oligomeric status. J. Appl. Physiol. **90**, 371–379
31 Froemming, G. R., Murray, B. E. and Ohlendieck, K. (1999) Self-aggregation of triadin in the sarcoplasmic reticulum of rabbit skeletal muscle. Biochim. Biophys. Acta **1418**, 197–205
32 Froemming, G. R. and Ohlendieck, K. (2001) The native dihydropyridine receptor exists as a supramolecular complex in skeletal muscle. Cell. Mol. Life Sci. **58**, 312–320
33 Bradd, S. J. and Dunn, M. J. (1993) Separation and analysis of membrane proteins by SDS–polyacrylamide gel electrophoresis. Methods Mol. Biol. **19**, 203–210
34 Campbell, K. P., MacLennan, D. H. and Jorgensen, A. O. (1983) Staining of the Ca^{2+}-binding proteins, calsequestrin, calmodulin, troponin C, and S-100, with the cationic carbocyanine dye 'Stains-all'. J. Biol. Chem. **258**, 11267–11273
35 Murray, B. E. and Ohlendieck, K. (1997) Cross-linking analysis of the ryanodine receptor and α_1-dihydropyridine receptor in rabbit skeletal muscle. Biochem. J. **324**, 689–696
36 Bradford, M. M. (1976) A rapid and sensitive method for the quantitation of microgram quantities of protein utilizing the principle of protein–dye. Anal. Biochem. **72**, 248–254
37 Glover, L., Quinn, S., Ryan, M., Pette, D. and Ohlendieck, K. (2002) Supramolecular calsequestrin complex. Eur. J. Biochem. **269**, 4607–4616
38 Sanchez, J. C., Chiappe, D., Converset, V., Hoogland, C., Binz, P. A., Paesano, S., Appel, R. D., Wang, S., Sennitt, M., Nolan, A., Cawthorne, M. A. and Hochstrasser, D. F. (2001) The mouse SWISS-2DPAGE database: a tool for proteomics study of diabetes and obesity. Proteomics **1**, 136–163
39 Dowling, P., Culligan, K. and Ohlendieck, K. (2002) Distal mdx muscle groups exhibiting up-regulation of utrophin and rescue of dystrophin-associated glycoproteins exemplify a protected phenotype in muscular dystrophy. Naturwissenschaften **89**, 75–88
40 Suk, J. Y., Kim, Y. S. and Park, W. J. (1999) HRC (histidine-rich Ca^{2+} binding protein) resides in the lumen of the sarcoplasmic reticulum as a multimer. Biochem. Biophys. Res. Commun. **263**, 667–671
41 Emery, A. E. (2002) The muscular dystrophies. Lancet **359**, 687–695
42 Monaco, A. P., Neve, R. L., Colletti-Feener, C., Bertelson, C. J., Kurnit, D. M. and Kunkel, L. M. (1986) Isolation of candidate cDNAs for portions of the Duchenne muscular dystrophy gene. Nature (London) **323**, 646–650
43 Hoffman, E. P. (1999) Muscular dystrophy: identification and use of genes for diagnostics and therapeutics. Arch. Pathol. Lab. Med. **123**, 1050–1052
44 Watchko, J. F., O'Day, T. L. and Hoffman, E. P. (2002) Functional characteristics of dystrophic skeletal muscle: insights from animal models. J. Appl. Physiol. **93**, 407–417
45 Turner, P. R., Schultz, R., Ganguly, B. and Steinhardt, R. A. (1993) Proteolysis results in altered leak channel kinetics and elevated free calcium in mdx muscle. J. Membr. Biol. **133**, 243–251
46 Robert, V., Massimino, M. L., Tosello, V., Marsault, R., Cantini, M., Sorrentino, V. and Pozzan, T. (2001) Alteration in calcium handling at the subcellular level in mdx myotubes. J. Biol. Chem. **276**, 4647–4651
47 Pandey, A. and Mann, M. (2000) Proteomics to study genes and genomes. Nature (London) **405**, 837–846
48 Isfort, R. J. (2002) Proteomic analysis of striated muscle. J. Chromatogr. B **771**, 155–165
49 Ohlendieck, K. and Campbell, K. P. (1991) Dystrophin constitutes 5 % of membrane cytoskeleton in skeletal muscle. FEBS Lett. **283**, 230–234

Received 27 August 2003/10 December 2003; accepted 16 December 2003
Published as BJ Immediate Publication 16 December 2003, DOI 10.1042/BJ20031311